Lithium isotopes in population II dwarfs

L. Piau[1]
CEA-Saclay DSM/IRFU/SAp, L'Orme des Merisiers, 91191 Gif-sur-Yvette, France

ABSTRACT

We address the evolution of lithium in Population II dwarf stars under the joint effects of microscopic diffusion and tachocline mixing. This process relies on analytical developments and is also constrained by helioseismology observations. It was successfully applied to solar analogs but never investigated in halo stars. It is induced in the upper radiation zone by rotation and a slight differential rotation in latitude. Consequently we modelled different possible rotation histories of halo stars showing that the initial rotation rate had no impact on lithium in the framework of tachocline mixing. We find a negligible impact of pre main sequence evolution on ^{7}Li independent of metallicity provided that [Fe/H] < -1. On the contrary microscopic diffusion and tachocline turbulence act on the long term of main sequence and shape the current $^7\mathrm{Li} - \mathrm{T_{eff}}$ pattern from the turn off down to 5000 K. The tachocline mixing models fit the ^{7}Li-$\mathrm{T_{eff}}$ relation better than the pure microscopic diffusion models.

We address the issue of warm ^{7}Li poor stars and conclude that a moderate mass transfer from a companion could explain their composition. Finaly we discuss the lithium lighter isotope. Pre main sequence and main sequence ^{6}Li depletion we compute seem difficult to reconcile with the current observations.

Subject headings: stars: Population II — stars: light elements — stars : internal mixing

1. Introduction

In standard Big Bang Nucleosynthesis (hereafter BBN), ^{7}Li is produced in an observable amount. Estimating its initial abundance from Population II dwarfs provides indications on the primordial Universe. In 1982 Spite & Spite (1982) found that most halo field stars with [Fe/H] < -1.5 and 5500K $< \mathrm{T_{eff}} <$ 6300K display similar ^{7}Li abundances. Since then this result was confirmed by many other observations (Ryan et al. 1996,1999, Bonifacio & Molaro 1997; Bonifacio et al. 2002; Asplund et al. 2006). The ^{7}Li abundance on the Spite plateau is now estimated to lie around 2.0-2.2 dex with a very small intrinsic scatter always found below 0.1 dex (Ryan et al. 1999; Asplund et al. 2006). In contrast to ^{7}Li, ^{6}Li is not significantly produced through standard BBN but results from fusion or spallation in the interstellar medium. His history gives indications on cosmic rays activity in the course of the Galaxy evolution. Although ^{6}Li abundance was already measured in Population II stars a decade ago (Cayrel et al. 1999; Nissen et al. 1999) the sample of objects where it has been probed and detected increased only recently (Asplund et al. 2005a, 2006).

Both lithium isotopes raise unsolved problems in Population II dwarfs. The flat and unscattered ^{7}Li plateau supports a cosmological origin. However with [^{7}Li] ~ 2.1 the plateau lies at least 0.5 dex below the standard BBN predictions (Spergel et al. 2007). There are furthermore a few stars having an even lower [^{7}Li] despite temperatures in the [5500K,6300K] range. ^{6}Li is also intriguing : present measurements suggest no evolution with metallicity which contradicts the pattern expected (Vangioni-Flam et al. 1999). The main factor for lithium evolution in halo stars is the microscopic diffusion (Salaris and Weiss 2001). Yet most authors compute that in order to obtain the plateau some kind of turbulent mixing below the convection zone must counteract the diffusive effects (e.g. Richard et al. 2005) and rotation effects appear as natural candidates for this turbulence

(Pinsonneault et al. 1992, 2002; Deliyannis & Pinsonneault 1997; Théado & Vauclair 2001). Other candidates to lithium depletion such as mass loss (Vauclair & Charbonnel 1995) or mixing by internal waves (Montalbán & Schatzman 2000) were also studied.

Here we study the joint impact of the microscopic diffusion and the tachocline mixing. The tachocline mixing is a rotationally induced instability occuring at the transition region between the radiative core and the convective enveloppe of solar like stars (Spiegel & Zahn 1992). This rotationally induced mixing has been successfully applied to the Sun and Population I where it fits ^{7}Li observed abundance and evolution (Brun et al. 1999 ; Piau et al. 2003). However the tachocline mixing was never investigated in Population II stars. We explore this effect under various rotation speeds during the main sequence (hereafter MS) because rotation history in Population II stars is unknown. We also consider the pre mainsequence (hereafter pre MS) evolution. We investigate the pre MS history for several metallicities as, in Population I solar like stars, the pre MS depletion is important and strongly metallicity dependent. Finaly we briefly touch on the question of ^{6}Li and address the question of the stars having an effective temperature above 6000 K but a ^{7}Li abundance clearly below the plateau.

We use recent physics in terms of nuclear reaction rates, equation of state and opacities. The paper is organized as follows: in §2 we describe the physical inputs to our code and the assumed initial compositions. In §3 we present our assumptions on the rotation and discuss the restrictions of our approach. Then we describe the modelling of the tachocline mixing process. Section 4 investigates the effects of pre MS and MS history on ^{7}Li. Section 5 addresses the question of ^{6}Li. We discuss our results and conclude in §6.

2. The evolutionary code and general inputs

We use the CESAM code (Morel 1997), an hydrostatic onedimensional code that has been extensively used to model various stellar types and stages of evolution over the last decade. It has also been used in solar structure computations and helio-/asteroseismology[1]. Different adaptations have been made to the code to address the curent issue.

The equation of state: we use the OPAL2001 EOS tables for pure hydrogen-helium mixtures [2] (Rogers & Nayfonov 2002).

The opacities: we use the α-element enhanced OPAL opacity tables tables with the composition recommended by F. Allard[2]. For these tables $[\alpha/\mathrm{Fe}] = 0.3$ dex where α stands for the α-elements (see hereafter). Table 1 resumes the heavy elements repartition assumed for the opacity calculations. Below log T =3.75, opacities are based on computations similar to those of Alexander and Ferguson (1994) and were provided by J. Ferguson (private communication). These tables were generated for the same intermetallic ratios as those of the OPAL opacity tables.

The nuclear reactions: we use the NACRE compilation of nuclear reaction rates (Angulo et al. 1999). Our network includes the proton-proton chains, the CNO cycle and the $^6\mathrm{Li}(\mathrm{p},\alpha)^3\mathrm{He}$ reaction.

The atmosphere modelling: the outer boundary conditions to the stellar structure equations are provided using the Phoenix NextGen atmosphere models from Hauschildt et al.[3]. The atmospheric temperature-optical depth relations have kindly been computed by P. Hauschildt for the required composition and on a grid that spans the effective temperature-surface gravity domain we encounter.

The convection: the convection zones are assumed to be fully homogeneous, and modeled using the mixing-length theory (hereafter MLT) in a formalism almost identical to that of Böhm-Vitense (1958). For a detailed description of this formalism see the appendix of Piau et al. (2005). We have considered $\alpha_{\mathrm{MLT}} = 1.766$ which is our Sun-calibrated value.

The diffusion and turbulence processes: the microscopic diffusion is taken into account following the Michaud & Proffitt (1993) prescription. No radiative levitation is accounted for. The turbulent

[1] A list of the scientific publications using this tool is available at http://www.oca.eu/morel/articles.html

[2] Available at http://www-physci.llnl.gov/Research/OPAL/

[3] Data from the Phoenix code available at ftp://phoenix.hs.uni-hamburg.de/

diffusion in the upper radiation zone is introduced following Spiegel & Zahn (1992). The turbulent diffusion term is adjusted by the differential rotation and buoyancy just below the base of the convection zone in the so-called tachocline region. This tachocline mixing is described in more details in section §3.

We assume [α/Fe]=+0.3. For Population II stars, this is the overabundance traditionally admitted in alpha elements (Ne,Mg,Si,S,Ar,Ca and Ti) and oxygen (see for instance Gratton et al. 2003). Besides this we consider [C/Fe]=0 and [N/Fe]=0 (Israelian et al. 2004). The total helium mass fraction along with the ratios of ^{2}H, ^{3}He, and ^{7}Li to ^{1}H are set to their primordial values following the recent standard BBN calculations of Coc et al. (2004). Given the most recent baryon number estimate (Spergel et al. 2007), the standard BBN predicts [^{6}Li] below -1 (Vangioni-Flam et al. 2000). The current ^{6}Li observations show a ^{6}Li abundance more than two orders of magnitude above the low BBN value in (some) Population II turn-off stars. The observations are around [^{6}Li]=1 and because ^{6}Li is only depleted in stars this suggests that it is more realistic to choose a higher than BBN value for the initial ^{6}Li abundance. We adopted [^{6}Li]=0.93 which is adapted from the observations of a turn-off Population II star of Cayrel et al. (1999) and is also in agreement with the recent observations of Asplund and collaborators. The tables 1 and 2 provide the detailed composition in heavy and light elements respectively. Hydrogen and helium mass fractions are X=0.7518 and Y=0.2479 respectively when [Fe/H]=-2. Unless explicitly mentioned we always adopt this composition.

3. The rotation: history and mixing effect

The tachocline mixing results from rotation. It is determined by the conditions around the base of the convection zone: the global rotation, the differential rotation with latitude and the stellar structure. We investigate various cases of rotation histories. We always assume that the star rotates as a solid except in one case where we considered distinct solid rotation in the radiative core and the convective envelope (see section 3.2). The differential rotation in latitude is deduced from the global rotation using a scaling law. Our approach of rotation neglects the internal transport of angular momentum and the (associated) radial differential rotation. In this respect it is less sophisticated than that of works specifically dedicated to rotation, e.g. by the Geneva group (Maeder and Meynet (2000) and references therein), or other approachs more focused on lithium: Pinsonneault et al. (2002) or Talon and Charbonnel (2004). Nevertheless there are hints that the angular momentum is not a relevant quantity for the history of light elements during the MS of low mass stars. Some indications come from the Population I and some from the Population II.

In Population I open clusters the lithium abundances of G dwarfs regularly decreases from M34 (250 Myr) age to solar age (Sestito & Randich 2005). However after the age of M34 and the Hyades, G dwarfs are slow rotators with respective equatorial velocities below 20 km/s and 10 km/s (Bouvier et al. 1997, hereafter BFA97). Furthermore tidally locked binary systems where angular momentum is conserved do not display anomalous lithium abundances (Balachandran 2000) with respect to single stars counterparts as wrongly suspected in the 1990s. This point cannot be explained if a strong connection exists between light element depletion and angular momentum loss.

In Population II stars the presence of a tight lithium plateau is also a support against a connection between lithium and angular momentum. The rotation history of Population II dwarfs can not be observed yet it is difficult to imagine how these stars could have had the same initial angular momentum. It seems more likely that they went through similar rotation histories as their Population I counterparts, having experienced very diverse rotation speeds on their zero age main sequence (hereafter ZAMS). These differences have not translated into different lithium abundances as the scatter on the lithium plateau -if any- is very low (Asplund et al. 2006).

So we focus here on the tachocline mixing due to the strong horizontal turbulence between the convection and the radiation zones. This phenomenon occurs in an object nearly rotating as a solid and is related to an only slight differential rotation with latitude in the surface convection zone as currently observed in the Sun. In order to evaluate the evolution of the global rotation rate we assume that the star rotates like a solid. Then

Table 1: Metal fractions relative to the Sun. We assumed the Grevesse and Noels (1993) solar composition.

Metals	[X/H]
O,Ne,Na,Mg,Si,P,S,Cl,Ar,Ca,Ti	-1.7
Fe,Ni,Cr,C,N,K	-2.0

Table 2: Light element number abundances relative to hydrogen adapted from Coc et. al (2004) except for ^{6}Li taken from Cayrel et al. (1999). Following Coc et al. (2004) we consider the helium mass fraction to be Y=0.2479.

ratios	^{2}H/^{1}H	^{3}He/^{1}H	^{6}Li/^{1}H	^{7}Li/^{1}H
values	$2.60\,10^{-5}$	$1.04\,10^{-5}$	$8.51\,10^{-12}$	$4.15\,10^{-10}$
values (log)	7.41	7.01	0.93	2.62

the differential rotation with latitude $\tilde{\Omega}$ necessary to the tachocline mixing calculation is estimated following a scaling law with the global rotation $\tilde{\Omega} \sim \Omega^{0.7}$ (Donahue, Saar & Baliunas 1996). $\tilde{\Omega}$ is not computed *in* the models where no differential rotation in latitude exists but is just a term taken into account in the turbulence generation. We calculated the history of rotation of a $0.7M_\odot$ model. With $T_{\rm eff} = 5890$K at 13 Gyr this star lies on the Li-plateau and is representative of most halo stars we are interested in.

Let us now give the ascribed rotation laws and describe in more details the tachocline mixing process.

3.1. The surface rotation

Currently all the main sequence Population II dwarfs exhibit very low equatorial velocities and we have no constrains on their surface rotation history. We assume that they experience the same evolution of surface rotation as their Population I counterparts:

i) The star initially rotates as a solid body and following BFA97 we consider an initial rotational period of $P_o = 8$ days. This period remains unchanged until the star decouples from its initial accretion disk which we assume occurs at τ_d =3 Myr (case A) or 0.5 Myr (case B).

ii) Once the star is no longer locked to its disk, the angular momentum decreases following the Kawaler (1988) prescription.

$$\frac{dJ}{dt} = -K\Omega^3 (\frac{R}{R_\odot})^{1/2} (\frac{M}{M_\odot})^{-1/2} \text{ if } \Omega < \Omega_{\rm sat} \quad (1)$$

$$\frac{dJ}{dt} = -K\Omega{\Omega_{\rm sat}}^2 (\frac{R}{R_\odot})^{1/2} (\frac{M}{M_\odot})^{-1/2} \text{ if } \Omega > \Omega_{\rm sat} \quad (2)$$

These laws are intended to describe the rotation braking through the magnetized wind of the star. K is set to $K_\odot = 3.25\,10^{47}$g.s.cm^2 (cases A and B) which leads to the actual solar rotation for a solar model. For case C we take $K = K_\odot/10$. This second value yields $1.6\,{\rm km\,s^{-1}}$ equatorial velocity at 13 Gyr which is nearly the maximum velocity allowed by current observations: studying 9 halo stars Smith et al. (1998) found vsini < 3km/s , a limit that was lowered to 2km/s by subsequent observations (Ryan et al. 2002). The surface magnetic activity saturates around $10\Omega_\odot$. The actual threshold $\Omega_{\rm sat} = 14\Omega_\odot$ ($3.78\,10^{-5}{\rm rad\,s^{-1}}$) is accurately tuned from the rotation observations in middle aged open-clusters (BFA97).

The four empirical parameters (P_o,τ_d, $\Omega_{\rm sat}$,K) in the rotation law we adopt are directly calibrated from the observations on our Sun and Population I solar analogs. It seems reasonable to assume similar angular momentum losses through magnetic braking for solar analogs and Li-plateau stars. The Sun is quite comparable to our $0.7M_\odot$ Population II [Fe/H]=-2 model. At 13 Gyr we find for this object : $T_{\rm eff} = 5890$ K, surface gravity = 1.36 $g_\odot$ and

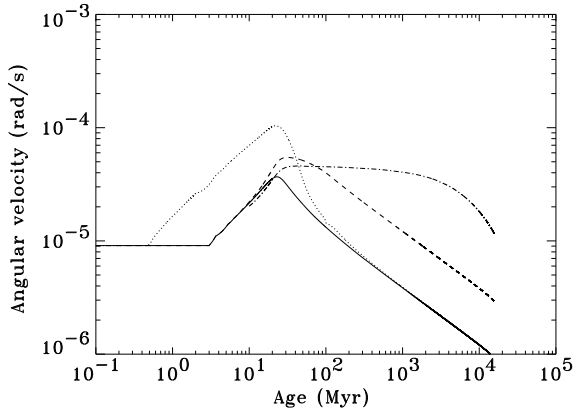

Fig. 1.— Radiation zone angular velocity vs age we calculated for a $0.7 M_\odot$ model. The solid body rotation models are shown by the solid line : $K = K_\odot$, and $\tau_d = 3$ Myr (case A); the dotted line : $K = K_\odot$, and $\tau_d = 0.5$ Myr (case B); the dashed line : $K = K_\odot/10$, and $\tau_d = 3$ Myr (case C). Dot-dashed line represents the differential rotation model with $K = K_\odot$, $\tau_d = 3$ Myr and $\tau_c = 1$ Gyr (case D). The difference between the case A and case B models is related to early conditions and vanishes after ~ 500 Myr.

0.764 $R_\star$ as radius for the radiative core vs 0.713 $R_\odot$ for the actual Sun (global properties of plateau stars as a function of their masses can be found in Proffitt & Michaud 1991). We consequently apply the braking law parameters from BFA97. The shorter P_o and/or τ_d the higher ZAMS rotation velocity (Figure 1). Then a higher Ω_{sat} implies a slower pace for rotational slow-down during the early MS. To study the effects of fast ZAMS rotation we built a model with $\tau_d = 0.5$ Myr. We stress however that none of the three parameters (P_o, τ_d and Ω_{sat}) has a significant impact on rotation after ~ 0.5 Gyr. In contrast, the K parameter determines the star's asymptotic velocity. Considering $\tau_d = 3$ Myr, when K changes from $K_\odot$ to $K_\odot/10$ the surface rotation velocity varies from ~ 0.6 to $\sim 1.7\,\mathrm{km\,s^{-1}}$ at 13 Gyr (Figure 1).

3.2. The internal rotation

The rotational rate in the upper radiation zone is the relevant quantity for the tachocline diffusion computation. In the case of Population I solar like stars solid body rotation is very likely during the MS: helioseismic observations show that our Sun rotates nearly as a solid at least down to $0.2 R_\odot$ (Couvidat et al. 2003, Garcia et al. 2008). Some recent models of angular momentum transport by internal waves suggest an efficient rigidification of the stellar interior both for the Sun (Talon, Kumar & Zahn 2002) and for the lithium plateau stars (Talon & Charbonnel 2004).

In the case of lithium plateau stars however we cannot completely exclude radial differential rotation because part of the low metallicity horizontal branch stars show significant surface rotation while on the other hand the turn off halo stars are slow rotators. We therefore built a rotation model (Case D) assuming $K = K_\odot$, $\tau_d = 3$ Myr and $\tau_c = 1$ Gyr. For this model the radiative core and the convective envelope rotate like solids but with different velocities. They exchange an angular momentum fraction $dJ = \frac{\Delta J}{\tau_c} dt$ during the time interval dt where:

$$\Delta J = \frac{(I_{env} J_{core} - I_{core} J_{env})}{I_{core} + I_{env}}$$

ΔJ is the angular momentum exchange that would achieve synchronization of the core and the envelope, τ_c is therefore a coupling timescale for rotation between these regions. As shown on Figure 1 this option yields to a significant increase of the rotation rate in the radiation zone. At 13 Gyr the core of the $0.7\,M_\odot$ star rotates at $1.35\,10^{-5}\,\mathrm{rad\,s^{-1}}$ while the surface rotation linear velocity at the equator is $1.5\,\mathrm{km\,s^{-1}}$. The total amount of angular momentum in this configuration is compatible with the observation of horizontal branch fast rotating stars (Behr 2003) if we consider the evolution of angular momentum during the red giant branch by Sills and Pinsonneault (2000).

So we explore 4 cases for the rotation:

Case A: solid body rotation: K is the constant for angular momentum loss, $K = K_\odot$, and τ_d is the initial circumstellar disk lifetime, $\tau_d = 3$ Myr. These parameters are calibrated thanks to the Sun and young Population I observations. Unless explicitly mentioned we will always use this rotational law.

Case B: solid body rotation, $K = K_\odot$, and $\tau_d = 0.5$ Myr.

Case C: solid body rotation, $K = K_\odot/10$, and

$\tau_d = 3$ Myr. Cases B and C evaluate the impact of increased rotation rates with respect to case A either because of lower angular momentum losses or higher ZAMS rotation speed.

Case D: model with differential rotation with depth $K = K_\odot$, and $\tau_d = 3$ Myr. The radiative core and convective envelope rotate like solids but with different velocities. The coupling time scale between the convective envelope and the radiative core is $\tau_c = 1$ Gyr. This model aims at evaluating the effects of a possible fast rotating core.

3.3. The tachocline mixing

The rotation and differential rotation with latitude induce a slow mixing below the base of the solar convection zone (Spiegel & Zahn 1992). This mixing can be described in a first order approximation by a turbulent coefficient term :

$$D_T(r) = \frac{1}{180}\frac{1}{4}\left(\frac{8}{3}\right)^2 \nu_H \left(\frac{d}{r_{BCZ}}\right)^2 \mu^6 Q^2 \exp(-2\zeta)\cos^2(\zeta)$$

with $Q = \tilde{\Omega}/\Omega$, $\mu = 4.933$, $\zeta = \mu(r_{BCZ} - r)/d$ and $d = r_{BCZ}(2\Omega/N)^{1/2}(4K/\nu_H)^{1/4}$. d is the width of the tachocline, ν_H is the horizontal viscosity, r is the radius, r_{BCZ} is the radius of the base of the convection zone (hereafter BCZ), N the Brunt-Väisälä buoyancy frequency and K the radiative diffusivity at BCZ.

Such a prescription has been introduced in modelling studies about the Sun and Population I solar-like stars (Brun et al. 1999; Piau & Turck-Chièze 2002, hereafter PTC 2002; Piau et al. 2003). It produces better agreement between theoretical and observed sound speed and explains the ^{7}Li and ^{9}Be main sequence histories. However, the tachocline mixing effect has never been systematically studied in Population II stars.

As mentionned above the tachocline mixing is not related to the internal angular momentum transport. Besides this and contrary to models where angular momentum is extracted by a diffusive process, it infers no ^{9}Be depletion in solar analogs. The prescription given above depends on two free parameters that must be empirically calibrated: the width of the tachocline (d) and buoyancy frequency (N) in the tachocline region. d is calibrated from solar seismic measurements to 2.5% of the total radius. This is the width of the region where the rotation goes from differential in latitude (in the convection zone) to solid body rotation (in the radiation zone). The value of the buoyancy frequency is estimated to be 10 μHz. A change to 2 μHz is investigated however (Figure 3). Near the top of the radiation zone the buoyancy frequency varies very rapidly with depth decreasing from a few hundreds of micro Hertz to zero at the border of the convection zone. A detailed discussion of our choice of buoyancy frequencies values can be found in Piau et al. (2003).

We neglect the tachocline mixing during the pre main sequence because the associated effective diffusion has a characteristic time scale of :

$$t_{diff} = 450(\frac{\tilde{\Omega}}{\Omega})^{-1}\text{Myr}$$

(Zahn 2004). Even in the case of extreme differential rotation ($\tilde{\Omega} = \Omega$) this duration is much longer than the pre main sequence.

4. Modelling the history of lithium 7

The deuterium abundance measurements in quasar absorption systems (Burles 2002 and references therein) and the cosmic microwave background anisotropies probed by the *Wilkinson Microwave Anisotropy Probe* point towards a similar ^{7}Li primordial fraction $[^7\text{Li}] \sim 2.6$ (Cyburt et al. 2003; Coc et al. 2004) i.e. 0.5 dex higher than what is observed in halo dwarfs of effective temperature larger than 5500 K (see Figure 2).

A lithium depletion during halo dwarfs evolution is a plausible explanation of this discrepancy. Yet the corresponding process has to comply with two challenges. First the plateau is remarkably flat with T_{eff}: stars with quite different outer convection zones experience similar depletion : Ryan et al. (1996) report a $\sim$ 0.04 dex ^{7}Li variation every hundred Kelvin. Second the scatter on the plateau is extremely small for field stars. e. g. Asplund et al. (2006) find $\sigma_{^7\text{Li}} \leq 0.02$ dex. Given the observational errors the scatter is generaly consistent with zero and in all recent studies clearly lies well below 0.1 dex [4].

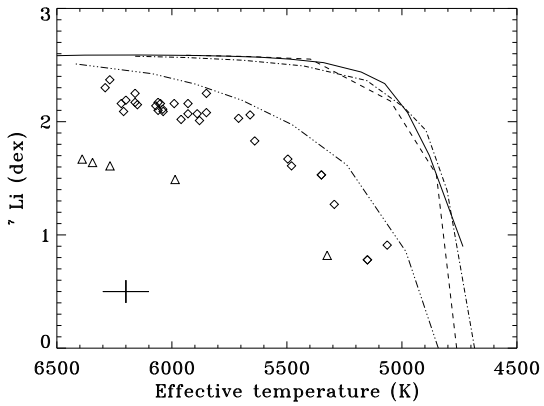

Fig. 2.— Models of ^{7}Li pre MS depletion at 200 Myr at [Fe/H]=-2 (solid line) , [Fe/H]=-1 (dashed line), [Fe/H]=-3 (dash-dotted line). These models exhibit similarly moderate pre MS ^{7}Li depletion patterns because the impact of metals on the metallicity is reduced. Accordingly the [Fe/H]=-0.7 models (dash three dotted line) exhibit higher depletion. Observations (diamonds) and upper limits (triangles) are from Ryan et al. (1996), Ryan & Deliyannis (1998), Ryan et al. (1999), Ryan et al. (2001) and Charbonnel & Primas (2005). Large error bars are shown on the lower left corner: $\Delta T_{\rm eff}$ = 100K, σ^7Li=0.1 dex. The very recent study of Asplund et al. (2006) rather suggest : $\Delta T_{\rm eff}$ = 30K, σ^7Li=0.026 dex.

4.1. The pre main sequence depletion

It is relevant to distinguish pre MS from MS depletion. The pre MS depletion is much faster and qualitatively different from the MS depletion because it is related to a major structural change in the stellar structure. During the pre MS, low mass stars presumably evolve from a fully convective state to a radiative core and convective envelope structure. The temperature at the BCZ reaches a maximum which may induce a rapid light elements depletion visible at the surface (Proffitt & Michaud 1989, Ventura et al. 1998, PTC02). The lower the mass (i.e. the lower the ZAMS $T_{\rm eff}$), the deeper the convection zone at any stage of the evolution and the stronger the light elements depletion. At 200 Myr the radiative core has reached its MS extension and the proton-proton chains provide more than 99% of the energy. Then the stars lie on the ZAMS and we therefore consider this age as the end of the pre MS. The computations were made for the helium mass fraction Y=0.2479 and the metallicities [Fe/H]=-3, [Fe/H]=-2 (standard case), [Fe/H]=-1 and [Fe/H]=-0.7.

As shown in Table 3 and Figure 2 no significant ^{7}Li depletion is induced during pre MS even for objects of ZAMS effective temperature at the cool end of the Spite plateau ($\sim 0.65 M_\odot$). Below this limit we estimate a depletion phenomenon rapidly increasing as the effective temperature decreases. These predictions are however unable to explain the $T_{\rm eff}$ $-^7$ Li pattern presently observed below 5500 K. Firstly in the $T_{\rm eff}$ $-^7$ Li plan, we compute a 0.18 dex ^{7}Li decrease per 100 K between 5175 K ($0.62 M_\odot$ model) and 4975 K ($0.58 M_\odot$ model). This slope is smaller than the estimate of 0.27 dex per 100 K based on observations between 5000 K and 5500 K suggested by Ryan & Deliyannis (1998). Secondly the predicted depletion rate around 5000 K is clearly lower than what is observed. One could object that in stars with $T_{\rm eff} < 5200$K the surface depletion started through convective mixing during the pre MS goes on during the MS by the same mechanism although with a much slower speed: our 0.58 $M_\odot$ purely diffusive model ($\sim$ 5000 K during the whole MS) depletes $\sim$ 0.5 dex during its first 200 Myr and $\sim$ 0.9 over the following 13 Gyr. In this effective temperature regime the gap between theory and observations decreases but -as illustrated by microscopic diffusion only models of the next section- remains significant even today.

We should conclude this section with a caveat. The pre MS depletion is unsure and varies in the different works of literature. Table 3 shows that our results stand in between the results of Salaris and Weiss (2001) who found larger depletions and those of Richard et al. (2005) who find smaller ones. The sensitivity of the pre MS depletion on the detailed physics of convection and opacities is well known (although mostly addressed in Population I stars) but there is a hint from Population I stars that the pre MS depletion is overestimated in the current modelling (Montalban & D'Antona (2006), D'Antona & Montalban (2003), PTC02, Ventura et al. 1998).

[4]The scatter observed in globular clusters such as M92 is higher (Boesgaard et al. 1998) and probably induced by the interactions resulting from the denser stellar environment.

Table 3: Lithium depletion in dex at the end of the pre MS as function of the effective temperature and at [Fe/H]=-2. In parenthesis are the effective temperatures at 13 Gyr. Compared with our calculations are those for pre MS of Salaris & Weiss (2001) line SW01 and Richard et al. (2005) line Ri05. Note that these authors considered [Fe/H]=-2.3 and their T_{eff} scale does not necessarily match ours.

Mass ($M_\odot$)	0.80	0.75	0.70	0.65	0.60	0.58
ZAMS T_{eff}(K)(13GyrT_{eff})	6144 (5784)	5893 (6237)	5621 (5887)	5341 (5499)	5072 (5117)	4975 (5002)
Δ^7Li_{ZAMS}	-0.013	-0.018	-0.031	-0.081	-0.263	-0.523
Δ^7Li_{ZAMS} SW01	-0.01	-0.02	-0.06	-0.21	-0.90	
Δ^7Li_{ZAMS} Ri05	∼0.0	∼0.0	-0.01	-0.03	-0.14	

4.2. The main sequence depletion

Pre main sequence computations suggest that the ^{7}Li abundance pattern was not achieved through early evolution. The objects having $T_{eff} > 5500$K at 13 Gyr experience a pre MS depletion of less than 0.08 dex. For cooler stars and down to 5000 K the pre MS depletion when added to the subsequent MS microscopic diffusion appears insufficent to explain the current abundances. As can be seen in Figure 3 at 5100 K the lithium abundance predicted by the models including only the microscopic diffusion is 2.2 dex at 13 Gyr. The pre MS depletion in the corresponding star (0.6 $M_\odot$) amounts to 0.26 dex (see table 3) and the diffusion and MS burning at BCZ do the remaining drop but the current observations are clearly below [^{7}Li]=1 around T_{eff} =5100 K. The pre MS depletion -as we compute it- can not fill the gap between microscopic diffusion only models and the observations.

In this section we investigate the effect of the MS tachocline mixing (Spiegel & Zahn 1992) on ^{7}Li. We compute the evolution of [Fe/H]=-2 models (detailed composition in tables 1 & 2). The rotation rate is a key parameter to the tachocline mixing (§3). Early rotation history has no impact on the MS tachocline mixing and on the surface lithium evolution. The reason stems from the swiftly converging rotational velocities after a few megayears combined with the few megayears the tachocline mixing requires for its onset (see §3). Despite probable differences in ZAMS angular momentum one does not expect a scatter in lithium on the plateau if the tachocline mixing is at play. Even if we exceptionally consider the effect of the tachocline mixing to start as early as 50 Myr, variations resulting from the early rotation differences (i.e. the different initial angular momentum amounts) would not be significant. In this situation the difference in ^{7}Li fraction we compute between the case of a slow and a fast ZAMS rotation (case A and B respectively on Figure 1) is 0.04 dex for the age 13 Gyr at T_{eff} = 5270 K and for a final ^{7}Li content of ∼0.0 dex. The differ-

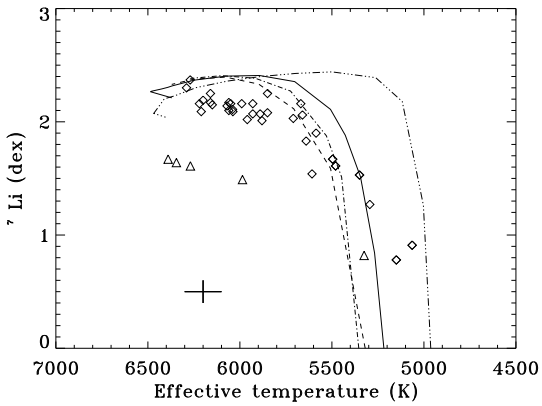

Fig. 3.— $T_{eff}-^7$Li relation in tachocline models for case A rotation history and for buoyancy frequency 10 μHz (solid line) and 2 μHz (dashed line) in the tachocline region. The ^{7}Li depletion pattern is also provided for case D rotation history and buoyancy frequency of 10 μHz (dot-dashed line) and pure microscopic diffusion models (dash-three dotted line). The age of the models is 13 Gyr, they all have the standard composition ([Fe/H]=-2). The data are the same as in figure 2.

ence of depletion gets smaller above this effective temperature. In the framework of our tachocline diffusion, the scatter in the lithium abundance between the case A and B rotation rates is negligible. We estimated ^{7}Li abundances for the case D rotation law to quantify the scatter induced by a possibly strongly enhanced rotation in the radiative core (see Figure 3). The rotation predicted in case D models is maximum as it assumes very weak losses of the radiation zone angular momentum. The associated tachocline impact is correspondingly close to the upper limit it may have in the case of fast rotating radiation zone: the difference in ^{7}Li depletion between case A and D rotations is around 0.4 dex at T_{eff}=5500 K but less than 0.1 dex above T_{eff}=5900 K. Figure 3 displays all these results. In order to diminish the possible ^{7}Li trends with [Fe/H] we selected stars with metallicity between -2.5 and -1.5 for the plateau objects ($T_{eff} \geq$ 5500K). Below T_{eff} = 5500K we use the data from Ryan & Deliyannis (1998), Thorburn (1994) and Charbonnel & Primas (2005). The sample of the seven objects below this temperature have a metallicity between -2 and -1. We selected dwarfs from this sample following Charbonnel and Primas (2005). Charbonnel and Primas (2005) work takes advantage of the HIPPARCOS parallaxes in determining the stellar evolutionary status.

The computations have been made with both tachocline and microscopic diffusion or microscopic diffusion only. In both cases a ^{7}Li plateau is predicted above 5500 K. This plateau lies between 0.2 and 0.4 dex below the initial abundances. Table 4 briefly provides a comparison at halo age of our pure diffusive models to those of Vauclair & Charbonnel (1998) (hereafter VC98). For similar effective temperatures ^{7}Li diffusion is similar except near the turn-off where VC98 find a 0.4 dex larger depletion. We suggest that this difference is due to our larger α_{mlt} = 1.766 parameter (vs α_{mlt} = 1.6 in VC98) which in turns induces shallower outer convection zones. VC98 do not mention their atmosphere boundary conditions and it is also possible that their larger depletion stems from a difference with ours. In our (purely) microscopic diffusion models the abundances decrease by 0.4 dex between 5700 K and the hotter end of the plateau at 6466 K. The ^{7}Li drop is very steep near the hotter edge of the plateau: [^{7}Li]=2.21 at 6356 K but [^{7}Li]=2.04 at 6466 K. The main effect of the tachocline mixing on the plateau is to correct this effective temperature dependence: a small decrease of 0.15 dex in ^{7}Li remains towards the hot edge. The calculated plateau peaks at 5900 K with [^{7}Li]=2.4 then the abundance falls at higher temperatures to 2.26 for 6500 K and at lower ones to 2.23 near 5400 K. On the plateau, the existence of correlations between ^{7}Li, T_{eff} and [Fe/H] are not settled yet. Here we restrict ourselves to compare our calculations with average plateau values. We just mention that while some observers do not find any significant ^{7}Li-temperature dependence (Bonifacio & Molaro (1997), Ryan et al. (1999), Asplund et al. (2006)) some other like Thorburn (1994) found a linear decrease of 0.2 dex with temperature from the turn off to 5600 K. The average [^{7}Li] plateau values generally reported ranges from 2.093 (Ryan et al. (1999)) to 2.21 (Asplund et al. (2006)). Slightly higher plateau values have been suggested : Thorburn's (1994) fit gives [^{7}Li]$\sim$2.3 when [Fe/H]=-2 while Melendez & Ramirez (2004) proposed [^{7}Li]=2.37 on the plateau. Our computations are in agreement with the predictions of Richard et al. (2005): on the one hand the microscopic diffusion plays the major role in determining the level of the plateau, on the other hand the shape of the plateau requires that a non standard mixing process occurs in the radiation zone. Above 6000 K the models buildt with the high rotation velocity of case D do not show differences in ^{7}Li exceeding 0.1 dex with the predictions of case A rotation models. In the framework of the tachocline mixing the most rapid rotation rates inferred from HB fast rotators are thus unable to explain the lithium poor stars near the turn off. We shall return to this question in the next chapter. Finaly we should mention that because of microscopic diffusion effects the heavy element fraction at 13 Gyr differs from the initial one. As expected, this phenomenon is maximum at turn-off for the models without any tachocline diffusion. For instance the oxygen fraction relative to hydrogen drops by 0.4 dex. Unfortunately iron being not included in our chemical network, we cannot properly comment on the variation of metallicity. However the calculations of Salaris et al. (2000) made with similar approximations suggest that the [Fe/H] variation should be moderate.

Table 4: Lithium depletion in dex for pure microscopic diffusion models of [Fe/H]=-2 at halo age and as function of the effective temperature. Compared with our calculations at 13 Gyr are those of Vauclair & Charbonnel (1998) adapted from their data at 12 Gyr. Note that these authors considered a smaller $\alpha_{\rm mlt}$ than we did.

This work $T_{\rm eff}$(K), Mass($M_\odot$)	6356, 0.77	6065, 0.725	5696, 0.675	5499, 0.65
This work Δ^7Li	-0.38	-0.26	-0.22	- 0.238
VC98 $T_{\rm eff}$(K), Mass($M_\odot$)	6322, 0.8	6044, 0.75	5723, 0.7	5392, 0.65
VC98 Δ^7Li	-0.76	-0.332	-0.19	-0.154

Right of the plateau, for models in the effective temperature range from 5700 K to 5200 K, the temperature of the BCZ during the MS is below $2.5\,10^6$ K. No ^{7}Li surface depletion occurs through convective mixing. Thus the pure microscopic diffusion models at [Fe/H]=-2 display a surface abundance in ^{7}Li that is high and almost independent of the temperature [^{7}Li]$\sim$2.4. The [^{7}Li] observed stand well below the computed values. This result is independent of metallicity. At 13 Gyr the pure microscopic diffusion models of [Fe/H]=-1 and $T_{\rm eff}$ of 5048 K (0.62 $M_\odot$) and 5623 K (0.7 $M_\odot$) respectively exhibit [^{7}Li]=1.54 and 2.32. All the observations we considered between 5500 K and 5000 K (in Figures 2 and 3) having metallicities between -1 and -2 the gap from theory to observations there cannot be ascribed to composition effects in microscopic diffusion models. On the contrary the tachocline mixing models provide a decrease of [^{7}Li] with temperature closer to observations. The tachocline mixing mimics a turbulent diffusion D_T in the upper radiation zone (D_T is given in section 3.3). This turbulence dredges the material below the BCZ in high temperature regions where ^{7}Li is destroyed by nuclear reactions. Figure 4 compares the ^{7}Li stratifications throughout the star for models with and without tachocline mixing and a $T_{\rm eff} \sim 5260$K. They differ only in the convection zone and the upper radiation zone. As the effective temperature decreases the BCZ reaches deeper, hotter regions and the ^{7}Li is ever more affected by tachocline mixing during the MS. Below $T_{\rm eff} \sim 5200$K the situation changes : the BCZ is hot enough and the surface ^{7}Li depletion occurs during the pre MS and the MS directly through convective mixing. Yet even after 13 Gyr the amount of depletion in pure microscopic diffusion models is insufficient to fit the observations between $T_{\rm eff} = 5200$K and 5000 K. The tachocline mixing therefore improves the situation with respect to pure microscopic diffusion models on the whole temperature range from 5700 K to 5000 K. We should add a caveat to this conclusion. The large differences between theory and observations below 5700 K are a priori sensitive to the choice of $\alpha_{\rm mlt}$ and the atmosphere boundary conditions. Moreover the observations are strongly dependent on the effective temperature scale. Thus it is possible that different models compared to different observations would not lead to the same conclusion.

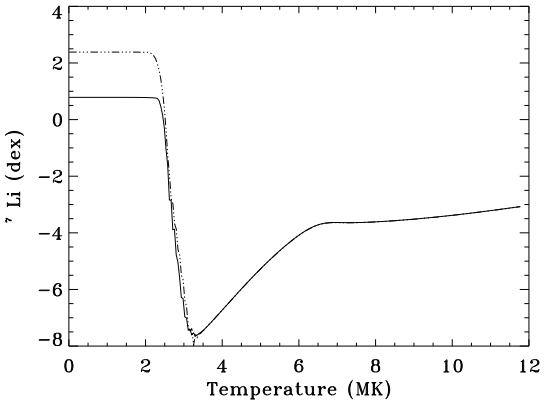

Fig. 4.— Temperature profile of ^{7}Li in a tachocline mixing model of 5268 K (solid line) and a pure microscopic diffusion model of 5262 K (three dot dashed line). The line styles are similar to figure 3. Both profiles are taken at 13 Gyr for 0.62 $M_\odot$ models of metallicity [Fe/H]=-2.

Although the tachocline models fit the observa-

tions better than the purely diffusive models the observed plateau still lies 0.2 dex below the predictions. A possible explanation of the discrepancy between the observed and predicted plateau may stem from an underestimation of [^{7}Li]. It has been suggested recently by Melendez & Ramirez (2004) that such an underestimate could be related to an incorrect evaluation of the T_{eff} scale (however see Asplund et al. 2006). The ^{7}Li plateau abundance infered by these authors is 2.37 dex which is in agreement with our predictions. Another explanation would be that some extra mixing destroys the lithium through nuclear reactions. To our knowledge the combined effects of several non standard mixing processes have not been explored. A last and more controversial explanation would be that the Population II stars we investigate simply did not formed from material having the standard BBN ^{7}Li fraction. Until recently most authors focused on lithium depletion mechanism occurring within the halo stars. In 2006, we explored a possible depletion of the primordial ^{7}Li induced by the first stars prior to the formation of the halo stars we currently observe (Piau et al. 2006). Such a decrease in the ^{7}Li initial content of halo stars could bring a better agreement between models and observations. See also Cumberbatch et al. (2007) for a possible solution of the issue related to particle physics.

4.3. Below the ^{7}Li plateau

About 7% of the halo turn-off stars are lithium poor with abundances below 1.7 dex (Spite et al. 1993; Ryan et al. 2002 and references therein). The majority of these stars clearly rotates faster than their Li-normal counter parts (Elliott & Ryan 2005). This could suggest a connection between lower lithium and faster rotation. However the distribution of rotational periods in ZAMS open-clusters such as IC2602 and IC2391 do not show a small fraction of stars, say between 5 and 10 %, having periods clearly shorter than the bulk of other comparable objects. It rather seems that rotation periods are uniformly distributed on the 0.2-10 days range (Barnes et al. 1999). If the ZAMS rotation distribution was responsible for lithium poor halo dwarfs at turn-off, one would expect more stars below the plateau and a continuous distribution of them as function of the lithium fraction. This is not the case: hot lithium poor stars are rare and there is an observational gap of objects between [^{7}Li] $\approx$ 2.1 dex and the upper limit of 1.7 dex. Table 5 shows the Ryan et al. (2002) data for their Li-poor stars. Out of the four objects of Table 5, CD-3119466 might be peculiar: it is neither a confirmed fast rotator nor a spectroscopic binary and is further away from turn-off than the other stars. On this basis we exclude it from the subsequent discussion

Our modelling suggests that none of pre MS depletion, MS tachocline mixing or microscopic diffusion are able to create the lithium poor (near) turn-off stars. Let us first consider the lower mass and higher metallicity models. They have deeper convection zones at any stage of the evolution and therefore get the maximum surface lithium depletion through nuclear destruction. During the pre MS, the depletion is related to the convection and during the MS, to the convection and the underlying tachocline mixing. At 13 Gyr a 0.77 $M_\odot$ and [Fe/H]=-1 model exhibits T_{eff} = 6113K. To be warmer at this age the Li poor stars displayed in Table 5 must either have a larger mass or a lower metallicity or both. Because of its mass and composition this model sets an upper limit to the nuclearly induced depletion around the turn-off. Its pre MS depletion of ~ 0.01 dex is totally negligible. The subsequent MS evolution including microscopic diffusion and tachocline mixing leads to [^{7}Li]=2.4 at 13 Gyr. For this calculation, the rotation rate has been considered constant on the MS at $1.27\,10^{-5}\mathrm{rad\,s^{-1}}$. At halo age this corresponds to an equatorial velocity of 8 $\mathrm{km\,s^{-1}}$ which is the order of the observed vsini for lithium poor warm stars (Table 5). If we now seek the maximum effects of microscopic diffusion we should consider the lower metallicity models of the previous section. None of these [Fe/H]=-2 models including purely microscopic diffusion lie below [^{7}Li]=1.9 at 13 Gyr when the effective temperature is higher than 6000 K.

Finaly if $-2 <$ [Fe/H] < -1, we do not predict Li abundances below 1.9 dex for any model of effective temperature above 6000 K and an age of 13 Gyr. Neither the uncertainties on metallicities (σ([Fe/H]) = 0.2) nor on the effective temperatures ($\sigma(T_{eff})$ = 125 K) are sufficient to recover the agreement between our calculations and the objects listed in Table 5. We suggest instead that the low lithium fraction in these stars is achieved

thanks to the accretion of lithium free matter. The Li-poor objects generally belong to binary systems. Indeed three out of four Li-poor stars of the Ryan et al. (2002) sample are confirmed binaries, the secondary component being presumably a compact object. This leads the authors to assume the higher rotation rates were achieved through angular momentum accretion accompanying a mass transfert from the former primary component. At the same time the accreted matter may have been initially lithium free and consequently induce dilution.

Let us consider the effect of dilution for a star of 0.8 $M_\odot$ having a metallicity of [Fe/H]=-1 and [^{7}Li]=2.1 at the surface before the accretion. Provided the convection zone of the star has the value of Table 6 a $1.4\,10^{-2}M_\odot$ mass transfert of lithium free material would be sufficient to dilute the ^{7}Li down to [^{7}Li]=1.6 dex. Alternatively if we consider an object of [Fe/H]=-2 and a total mass of 0.77 $M_\odot$ then a $3.2\,10^{-3}M_\odot$ accreted mass is enough to decrease the abundance to [^{7}Li]=1.6 dex. Given the small masses of the convection zones, moderate accretion can explain the low lithium surface abundances observed in some turn-off halo dwarfs. We furthermore remark that the models in Table 6 are slightly cooler than the objects of Table 5 and therefore should have heavier convection zones. Therefore the mass transfer we computed are in some sense maximum requirements for the observed dilution.

The need for an additive destruction process of ^{7}Li is required only if the accreted mass is below $10^{-3}M_\odot$. In this case the process responsible for the depletion could not possibly be the tachocline mixing as we show above. Abundance measurements of other elements than ^{7}Li would certainly clarify the issue of the origin of near turn-off ^{7}Li deficient stars. For instance the detection of higher nitrogen and lower carbon fractions than in the 'normal' halo dwarfs would support the accretion scenario from a red giant star. The conversion of carbon into nitrogen is ascribed to the first dredge-up at the bottom of the RGB and subsequently to deep mixing and is clearly observed from moderately (Smith, Briley & Harbeck 2005) to extremely (Spite et al. 2005) metal poor giants.

5. What about lithium 6?

^{6}Li is destroyed at $2\,10^6$ K vs $2.5\,10^6$ K for ^{7}Li. Thus it provides complementary informations about the internal structure and mixing. Our modelling of pre MS history of ^{6}Li suggests features whose consequences are not observed at 13 Gyr. First the depletion increases for decreasing effective temperature in the [6500,6000]K range. The observations show no such trend and also systematically suggest a higher abundance than predicted (Figure 5). Second because the outer convection zones extend closer to the ^{6}Li than the ^{7}Li burning regions the ^{6}Li depletion depends on metallicity between [Fe/H]=-2 and [Fe/H]=-1 (Michaud & Proffitt (1989) illustrated this in the context of Population I stars). On Figure 5 the coolest object (HD68284) and the object closest to 6000 K (HD160617) have respective metallicities of -0.59 and -1.76 and yet display similar ^{6}Li abundances. We expect a variation above 1.5 dex in ^{6}Li for a change Δ[Fe/H] = 1 if $T_{\rm eff} \leq 6000$K. Unless the early Galaxy ^{6}Li abundance was up to 2 dex and strongly varied from place to place we conclude that the ^{6}Li pre MS depletion is overestimated by the models. This parallels the issue of pre MS ^{7}Li overdepletion in Population I stars pointed out by many authors (Ventura et al. 1998, PTC02, D'Antona & Montalban 2003) and suggests the convection is less efficient in young stars.

Figure 5 also compares the ^{6}Li data to MS calculations. Not all the data correspond to confirmed dwarfs in the recent analysis of Charbonnel & Primas (2005). Yet the subgiants of the sample all are hot enough that no significant dilution or nuclear destruction is expected from deeper convection zones. Partly because of pre MS depletion, the predictions at current halo age are well below the observations. Quantitatively the ^{6}Li predictions are worse than the ^{7}Li predictions when it comes to observations. The presence of ^{6}Li in stars as cool as 5900 K appears really problematic. Qualitatively one can note several interesting features. Because the turbulence induced by the tachocline models is shallow, it brakes the diffusion of heavy elements around the turn-off without inducing nuclear destruction. Nevertheless below 6100 K the tachocline mixing enters regions where ^{6}Li is nuclearly destroyed and the tachocline

Table 5: Turn off lithium poor objects. Data from Ryan et al. (2001) and Ryan et al. (2002). These stars appear in Figure 2 and 3. Charbonnel & Primas (2005) showed that Wolf 550 is a dwarf and G202-65 is a subgiant. The evolutionary status of the two other stars are not mentioned by this work.

Object	vsini ($km\,s^{-1}$)	T_{eff} (K)	[Fe/H] (dex)	^{7}Li (dex)
CD-31 19466	< 2.2	5986	-1.66	< 1.49
Wolf 550	5.5 ± 0.6	6269	-1.56	< 1.61
BD +51 1817	7.6 ± 0.3	6345	-0.88	< 1.64
G202-65	8.3 ± 0.4	6390	-1.32	< 1.67

Table 6: Models characteristics at their turn off effective temperature.

Mass and metallicity ($M_\odot$)	T_{eff} (K)	age (Gyr)	Mass of the convection zone ($M_\odot$)
0.80 [Fe/H]=-1	6233	12.15	$6.5\,10^{-3}$
0.77 [Fe/H]=-2	6359	13.17	$1.5\,10^{-3}$

models deplete more ^{6}Li than the purely diffusive models. This phenomenon can be seen in the change of slope around this temperature in the tachocline mixing models of Figure 5. On Figure 6 the ratio ^{6}Li/^{7}Li is practically unchanged between tachocline and diffusive models above 6000 K but drops faster for tachocline models below this temperature. Provided that very small ^{6}Li/^{7}Li ratio can be observed this could be used to distinguish tachocline from diffusive models.

Currently no conclusion can be drawn about ^{6}Li and internal mixing during MS because the ^{6}Li pre MS is very strong and metallicity dependent. This should have left prints that clearly are not observed in the abundance pattern. As long as ^{6}Li is not understood during the pre MS it is dangerous to use it as a chemical probe for the subsequent evolution. Finaly we remark that the current data sample (Figure 5) mostly relies on measurements of Asplund et al. (2005a) where only 9 out of 24 stars yielded to unambiguous ^{6}Li detection. The estimate of the ^{6}Li/^{7}Li ratio depends on the process of line broadening in convective atmospheres that is still a matter of investigation (Cayrel et al. 2007). The current ^{6}Li measurements need to be confirmed and could actually turn out to be upper limits.

6. Summary

Lithium 7 observations are well constrained and this isotope in halo dwarfs is the main focus of this work. During the pre MS the peak temperature near the base of convection zones is too low to affect the ^{7}Li abundance of stars currently on the Spite plateau or having effective temperatures slightly lower say between 5500 and 5100 K. We compute that no significant pre MS depletion occurs in these objects. Thus the pre MS evolution cannot explain the current observations independently of the metallicity between -1 and -3 (§4). This point is connected to the waning influence of metals on opacity near the base of the convection zone for [Fe/H] < -1. The absence of metallicity dependence of the pre MS depletion strongly differs from the Population I situation.

We investigated the impact of the tachocline mixing during the MS. The tachocline mixing is a rotationally induced mixing that was tested in the case of the Sun and Population I stars but never in Population II stars. This process relies on analytical developments and is constrained by heliosismic observations. The corresponding models produce a flat ^{7}Li plateau from 5500 K up to the turnoff but also predict a strong decrease in ^{7}Li below

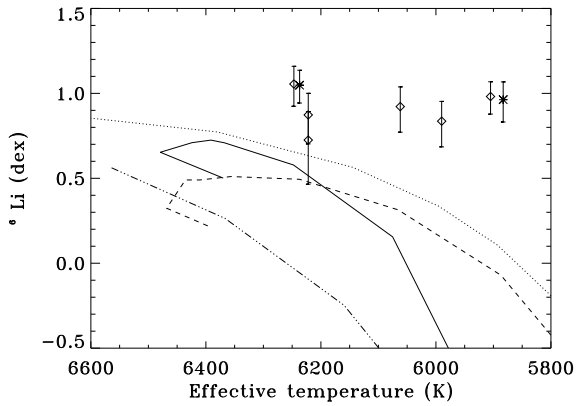

Fig. 5.— Solid line : T_{eff} $-^6$ Li relation for tachocline diffusion models of buoyancy frequency 10μ Hz and [Fe/H]=-2 at 13 Gyr. Dashed line : microscopic diffusion models for the same age and composition. The tachocline mixing brakes surface depletion only above 6100 K. Also shown are the pre MS depletion patterns at 200 Myr for [Fe/H]=-2 (dotted-line) and [Fe/H]=-1 (three dot dashed-line). Note the strong metallicity dependence of pre MS ^{6}Li dependence. The data and error bars are from Asplund et al. (2005a) (diamonds) and Nissen et al. (1999) (star symbols).

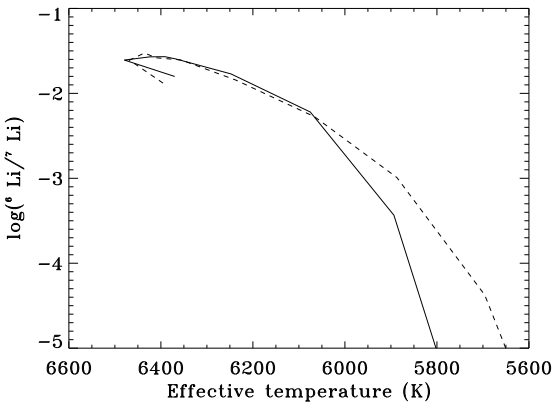

Fig. 6.— ^{6}Li/^{7}Li ratio vs effective temperature from tachocline models (solid line) and purely diffusive models (dashed line).

5500 K in agreement with the observations (§4). Purely microscopic diffusive models fail to complete these two points : they predict no significant lithium 7 depletion down to an effective temperature of 5100 K. The tachocline turbulence properly increase the nuclear destruction at the cool edge of the plateau and blocks microscopic diffusion at the hot edge (§4). We showed that although the tachocline mixing is generated by the rotation its impact on lithium is not sensitive to the early rotation history. The tachocline mixing affects the star on the long term when the rotation regimes all converge to similar speeds. The tachocline mixing predicts a plateau 0.2 dex higher than the bulk of observations. Another internal mixing process is a priori required to explain this moderate discrepancy unless the Population II initial [^{7}Li] actually differs from the primordial [^{7}Li]. We investigated the warm ($T_{eff} > 6000$K) ^{7}Li depleted objects. In spite of their fast rotation rates the additional ^{7}Li depletion is not related to a stronger internal mixing -at least in the framework of the tachocline mixing-. We showed that given the small mass of the convection zones of these objects (at most $10^{-2}M_\odot$) a moderate mass transfer of ^{7}Li free matter from an evolved companion would suffice to explain the observations. The detection of an enhanced nitrogen content in these objects would be a strong support for such an accretion scenario.

Lithium 6 observations are scarce and much more recent than observations of lithium 7. An interesting point is that similarly to ^{7}Li in Population I, the pre MS depletion of ^{6}Li in Population II appears too strong unless ^{6}Li was massively produced up to [^{6}Li] = 2 in the early Galaxy. This suggests that there is a common physical process blocking deep mixing in pre MS Population I and Population II stars. The MS evolution of ^{6}Li appears problematic for tachocline models below 6000 K. When put together lithium 7 and 6 raise a new modelling/theoretical issue : turbulence below the base of the convection zone is required to explain the ^{7}Li pattern but at the same time destroys too much ^{6}Li. However the ^{6}Li observations still need to be confirmed on an extended sample.

The author thanks the anonymous referee for his detailed review of this work and for useful remarks that helped to improve it. The author, currently working in the UMR7158 unit, acknowledges support from the Centre National de la Recherche Scientifique.

REFERENCES

Alexander, D. R., Ferguson, J. W., 1994, ApJ, 437, 879

Angulo, C., et al., Nucl. Phys. A656 (1999)3-187

Asplund, M., Nissen, P. E., Lambert, D. L., Primas, F., Smith, V. V., 2005a, Proceedings of IAU symposium 228, Ed. V. Hill, P. François, F. Primas.

Asplund, M., Grevesse, N., Sauval, A. J., 2005b, Cosmic Abundances as Records of Stellar Evolution and Nucleosynthesis, ASP Conference Series, Vol. XXX, 2005, F. N. Bash and T. G. Barnes Eds.

Asplund, M., Nissen, P. E., Lambert, D. L., Primas, F., Smith, V. V., 2006, ApJ, 644, 229

Balachandran, S., 2000, Highlights of Astronomy, Vol. 12, as presented at the XXIVth General Assembly of the IAU. Ed. H. Rickman. San Francisco, CA: PASP, 2002, p.276 - 278

Barnes, S. A., Sofia, S., Prosser, C. F., Stauffer, J. R., 1999, ApJ, 516, 263

Behr, B. B., 2003, ApJSS, 149,67

Boesgaard A. M., Deliyannis, C. P., Stephens, A., King, J. R., 1998, ApJ 493, 206

Böhm-Vitense, E., 1958, Zs. f. Ap., 46, 108

Bonifacio, P., Pasquini, L., Spite, F., Bragaglia, A., Carretta, E., Castellani, V., Centurin, M., Chieffi, A., Claudi, R., Clementini, G., and 9 coauthors, 2002, A&A, 390, 91

Bonifacio, P., Molaro, P., 1997, MNRAS, 285, 847

Bouvier, J., Forestini, M., Allain, S., (BFA97) 1997, A&A, 326, 1023

Brun, A. S., Turck-Chièze, S., Zahn, J. P. 1999, ApJ, 525, 1032

Burles, S., 2002, P&SS, 50, 1245

Cayrel, R., Spite, M., Spite, F., Vangioni-Flam, E., Cass, M., Audouze, J., 1999, A&A, 343, 923

Cayrel, R., Steffen, M., Chand, H., Bonifacio, P., Spite, M., Spite, F., Petitjean, P., Ludwig, H.-G., Caffau, E., 2007, A&A, 473, L37

Charbonnel, C., Primas, F., 2005, A&A, 442, 961

Coc, A., Vangioni-Flam, E., Descouvemont, P., Adahchour, A., Angulo, C., 2004, ApJ, 600, 544

Couvidat, S., Garca, R. A., Turck-Chize, S., Corbard, T., Henney, C. J., Jimnez-Reyes, S., 2003, ApJ, 597, L77

Cumberbatch, D., Ichikawa, K., Kawasaki, M., Kohri, K., Silk, J., Starkman, G. D., 2007, PhRvD, 76, 123005

Cyburt, R. H., Fields, B. D., Olive, K. A., 2003, Phys. Lett. B, 567, 227

D'Antona, F., Montalbán, J., 2003, A&A, 412, 213

Deliyannis, C. P.; Pinsonneault, M. H., 1997, ApJ, 488, 836

Donahue, R. A., Saar, S. H., Baliunas, S. L., 1996, ApJ, 466, 384

Elliott, L. M., Ryan, S. G., 2005, IAUA, 228, 91

Fabbian, D., Asplund, M., Calrsson, M., Kiselman, D., 2005, Proceedings of IAU Symposium 228 "From Li to U: Elemental Tracers of Early Cosmic Evolution", eds. V. Hill, P. Francois and F. Primas, Cambridge University Press.

Frebel, A., Aoki, W., Christlieb, N., Ando, H., Asplund, M., Barklem, P. S., Beers, T. C., Eriksson, K., Fechner, C., Fujimoto, M. Y., and 9 coauthors, 2005, Nature,434, 871

Garcia, R. A., Mathur, S., Ballot, J, 2008, Sol. Phys., 55

Gratton, R. G., Carretta, E., Desidera, S., Lucatello, S., Mazzei, P., Barbieri, M., 2003, A&A, 406, 131

Grevesse, N., and Noels A., 1993 in 'In Origin and Evolution of the Elements', eds.Prantzos, N., Vangioni-Flam, E. and Cass, M (Cambridge: Cambridge Univ. Press).

Hobbs, L. M., Duncan, D. K., 1987, ApJ, 317, 796

Iglesias, C. A., & Rogers, F., J., 1996, ApJ, 464, 943

Israelian, G., Ecuvillon, A., Rebolo, R., Garca-Lpez, R., Bonifacio, P., Molaro, P., 2004, A&A, 421, 649

Kawaler, S. D., 1988, ApJ, 333, 236

Maeder, A., Meynet, G., 2000, ARAA, 38, 143

Melendez, J., Ramirez, Y, 2004, ApJ, 615, 33

Michaud, G., Proffitt, C. R., 1989, ApJ, 346, 976

Michaud, G., Proffitt, C. R., 1993, Inside the stars , IAU colloquium, 137, ASP Conference series, eds. A. Baglin, & W. W. Weiss vol 40, 426

Montalbán, J. & Schatzman, E., 2000, A&A 354, 943

Montalbán, J., D'Antona, F., 2006, MNRAS, 370, 1823

Morel, P., 1997, A&AS, 124, 597

Nissen, P. E., Lambert, D. L., Primas, F., Smith, V. V., 1999, A&A, 348, 211

Piau, L., & Turck-Chièze, S., (PTC02) 2002, ApJ, 566, 419

Piau, L., Randich, S., & Palla, F., 2003, A&A, 408, 1037

Piau, L., Ballot, J., & , Turck-Chièze, S., 2005, A&A, 430, 571

Piau, L., Beers, T. C., Balsara, D. S., Sivarani, T., Truran, J. W., Ferguson, J. W., 2006, ApJ, 653, 300

Pinsonneault, M. H., Deliyannis, C. P., Demarque, P., 1992, ApJS, 78, 179

Pinsonneault, M. H., Steigman, G., Walker, T. P., Narayanan, V. K., 2002, ApJ, 574, 398

Primas, F., Molaro, P., Bonifacio, P., Hill, V., 2000, A&A, 362, 666

Proffitt, C. R., Michaud, G., 1991, ApJ, 371, 584

Proffitt, C. R., Michaud, G., 1989, ApJ, 346, 976

Richard, O., Michaud, G., Richer, J., 2005, ApJ, 619, 538

Rogers, F. J., Nayfonov, A., 2002, ApJ, 576, 1074

Ryan, S. G., Beers, T. C., Deliyannis, C. P., Thorburn, J. A., 1996, ApJ 458, 543

Ryan, S. G., Deliyannis, C. P., 1998, ApJ, 500, 398

Ryan, S. G., Norris, J. E., Beers, T. C., 1999, ApJ, 523, 654

Ryan, S. G., Kajino, T., Beers, T. C., Suzuki, T. K., Romano, D., Matteucci, F. Rosolankova, K., 2001, ApJ 549, 55

Ryan, S. G., Gregory, S. G., Kolb, U., Beers, T. C., Kajino, T., 2002, ApJ, 571, 501

Salaris, M., Groenewegen, M. A. T., Weiss, A., 2001, A&A, 355, 299

Salaris, M., Weiss, A., 2001, A&A, 376, 955

Sestito, P., Randich, S., 2005, A&A, 442, 615

Sills, A. Pinsonneault, M. H., 2000, ApJ, 540, 489

Smith, V. V., Lambert, D. L., Nissen, P. E., 1998, ApJ, 506, 405

Smith, G. H., Briley, M. M., Harbeck, D., 2005, AJ, 129, 1589

Spergel, D. N., Bean, R., Dor, O., Nolta, M. R., Bennett, C. L., Dunkley, J., Hinshaw, G., Jarosik, N., Komatsu, E., Page, L., and 12 coauthors, 2007, ApJS, 170, 377

Spiegel, E. A., Zahn, J.P., 1992, A&A, 265, 106

Spite, F., Spite, M., 1982, A&A 115, 457

Spite, M., Molaro, P., Francois, P., Spite, F., 1993, A&A, 271, L1

Spite, M., Cayrel, R., Plez, B., Hill, V., Spite, F., Depagne, E., Franois, P., Bonifacio, P., Barbuy, B., Beers, T., and 4 coauthors, 2005, A&A, 430, 655

Talon, S., Kumar, P., Zahn, J. P., 2002, ApJ, 574, 175

Talon, S., Charbonnel, C., 2004, A&A, 418, 1051

Théado, S., & Vauclair, S., 2001, A&A, 375, 70

Thompson, M. J., Christensen-Dalsgaard, J., Miesch, M. S., Toomre, J., 2003, A&ARA, 41, 599

Thorburn, J. A., 1994, ApJ, 421, 318

Vangioni-Flam, E., Cassé, M., Cayrel, R., Audouze, J., Spite, M., Spite, F., 1999, NewA, 4, 245

Vangioni-Flam, E., Coc, A., Cassé, M., 2000, A&A, 360, 15

Vauclair, S., Charbonnel, C, 1995, A&A, 295, 715

Vauclair, S., Charbonnel, C, 1998, ApJ, 502, 372

Ventura, P. Zeppieri, A., Mazzitelli, I., D'Antona, F., 1998, A&A, 331, 1011

Zahn, J. P. , 2004, 'Hydrodynamic models of the tachocline', Cambridge University press.

This 2-column preprint was prepared with the AAS LaTeX macros v5.2.